# Cardiac-Specific Nkx2.5 Homeodomain: Conformational Stability and Specific DNA Binding of Nkx2.5(C56S)†

Elfrieda Fodor,‡,§ James W. Mack,||,⊥ Jin-Soo Maeng,||,⊥ Jeong-Ho Ju,|| Hyun Sook Lee,|| James M. Gruschus,|| James A. Ferretti,|| and Ann Ginsburg*,‡

*Section on Protein Chemistry, Laboratory of Biochemistry, and Laboratory of Biophysical Chemistry, National Heart, Lung and Blood Institute, National Institutes of Health, Bethesda, Maryland 20892, and Department of Biochemistry and Molecular Biology, Howard University, Washington, D.C. 20059*

*Received May 5, 2005; Revised Manuscript Received July 20, 2005*

ABSTRACT: The cardiac-specific Nkx2.5 homeodomain has been expressed as a 79-residue protein with the oxidizable $Cys^{56}$ replaced with Ser. The Nkx2.5 or Nkx2.5(C56S) homeodomain is 73% identical in sequence to and has the same NMR structure as the vnd (ventral nervous system defective)/NK-2 homeodomain of *Drosophila* when bound to the same specific DNA. The thermal unfolding of Nkx2.5-(C56S) at pH 6.0 or 7.4 is a reversible, two-state process with unit cooperativity, as measured by differential scanning calorimetry (DSC) and far-UV circular dichroism. Adding 100 mM NaCl to Nkx2.5(C56S) at pH 7.4 increases $T_m$ from 44 to 54 ± 0.2 °C and $\Delta H$ from 34 to 45 ± 2 kcal/mol (giving a $\Delta C_p$ of ∼1.2 kcal $K^{-1}$ $mol^{-1}$ for homeodomain unfolding). DSC profiles of Nkx2.5 indicate fluctuating nativelike structures at <37 °C. Titrations of specific 18 bp DNA with Nkx2.5(C56S) in buffer at pH 7.4 with 100 mM NaCl yield binding constants of $2-6 \times 10^8$ $M^{-1}$ from 10 to 37 °C and a stoichiometry of 1:1 for homeodomain binding DNA, using isothermal titration calorimetry. The DNA binding reaction of Nkx2.5 is enthalpically controlled, and the temperature dependence of $\Delta H$ gives a $\Delta C_p$ of −0.18 ± 0.01 kcal $K^{-1}$ $mol^{-1}$. This corresponds to 648 ± 36 Å$^2$ of buried apolar surface upon Nkx2.5(C56S) binding duplex B-DNA. Thermodynamic parameters differ for Nkx2.5 and vnd/NK-2 homeodomains binding specific DNA. Unbound NK-2 is more flexible than Nkx2.5.

Homeodomains are an important class of DNA binding proteins that regulate embryonic development. Members of the homeodomain family have a high degree of homology in their tertiary structures and contain three helical segments (*1*). The C-terminal helix III recognizes DNA base pairs in the major groove, and the partially flexible N-terminal arm binds to the adjacent minor groove of DNA. Despite their similarities in structure, each homeodomain has a unique function in vivo when part of a full-length transcription factor.

The *Drosophila* NK homeodomains play essential roles in embryo development (*2*) and, like thyroid transcription factor-1 (TTF-1),[1] recognize the 5′-CAAG-3′ instead of the more commonly recognized 5′-TAAT-3′ DNA sequence (*3*−*5*). Molecular biologists interested in the DNA binding specificity and affinity of homeodomains typically use gel shift assays to measure these properties. However, this method gives only an estimate of binding affinity and no information about the temperature dependence of DNA binding or relative contributions of binding enthalpies and entropies. Only a few laboratories have reported thermodynamic parameters for both homeodomain unfolding/folding and DNA binding (*6*, *7*), and others have reported homeodomain unfolding while measuring DNA binding by gel shift assays (*8*, *9*). Many temperature-sensitive mutants of homeodomains have been identified (*10*−*13*), but they remain uncharacterized because thermodynamic data are unavailable. For example, the R52H mutation in the even-skipped homeodomain from *Drosophila* is lethal to embryo development at 30 °C but not at 20 °C, whereas development of wild-type embryos proceeds normally at both temperatures (*14*). Another example is the H52R mutation in the homeobox part of the *vnd/NK-2* gene. The R52 vnd/NK-2 protein is thermally more stable than the corresponding wild type and is structurally better behaved during thermally induced unfolding (*7*) and as determined by NMR criteria

† This work was supported by the Intramural Research Program of the NIH, NHLBI and by MBRS Grant GM 80615 (J.-S.M. and J.W.M.) and RCMI Grant G12 RR003048 (J.W.M.).

* To whom correspondence should be addressed: Section on Protein Chemistry, NHLBI/NIH, Building 50, Room 2339, Bethesda, MD 20892-8012. Telephone: (301) 496-1278. Fax: (301) 480-5492. E-mail: ginsbura@nhlbi.nih.gov.

‡ Section on Protein Chemistry, Laboratory of Biochemistry, National Heart, Lung and Blood Institute, National Institutes of Health.

§ All thermodynamic and fluorescence studies were performed by E.F., the primary contributor.

|| Laboratory of Biophysical Chemistry, National Heart, Lung and Blood Institute, National Institutes of Health.

⊥ Howard University.

[1] Abbreviations: NKX2.5, cardiac-specific homeodomain from human (CSX/NKX2.5); Nkx2.5, cardiac-specific homeodomain from mouse (Csx/Nkx2.5); vnd/NK-2, ventral nervous system defective/NK-2 homeodomain from *Drosophila melanogaster*; Bcd-HD, *Drosophila* Bicoid homeodomain; TTF-1, thyroid transcription factor 1; Tbx5, T-box transcription factor; GATA-4, zinc finger transcription factor; HD, homeodomain; MOPS, 3-(*N*-morpholino)propanesulfonic acid; MES, 2-(*N*-morpholino)ethanesulfonic acid; CD, circular dichroism; DSC, differential scanning calorimetry; ITC, isothermal titration calorimetry.

10.1021/bi050835s CCC: $30.25 © 2005 American Chemical Society
Published on Web 08/26/2005

(*10*). Nevertheless, transgenic experiments using the code for R52 result in embryonic toxicity as soon as mRNA expression is initiated, whereas in control experiments where the code for H52 is present, normal embryonic development occurs (K. Koizumi and J. A. Ferretti, unpublished observations). Some of the effects described above may be caused by defects in protein−protein interactions during transcription rather than in DNA interactions. Nevertheless, Subramaniam et al. (*9*), for example, have determined that W48F or F8A mutants of the *Drosophila* Bicoid (Bcd) homeodomain are destabilized relative to the wild-type Bcd-HD and also have lost the ability to bind to DNA.

The *CSX/NKX2.5* homeobox is one of the earliest genes expressed during cardiac development in both mice and humans (*15*, *16*). The gene product regulates atrial septation and left ventricle formation, and continues to be expressed in the heart throughout life (*17*). Various congenital heart diseases in humans are linked to the presence of single-amino acid residue replacements due to different mutations in the *NKX2.5* homeobox itself (*18*−*21*). How these mutations lead to cardiac defects is still unknown; however, it can be predicted that they may alter the protein stability and protein−protein interactions with other transcription factors (such as Tbx5 and GATA-4) and/or impair or abolish target-DNA binding of the expressed homeodomain protein. The homeodomain segment of the mouse Nkx2.5 (known as Csx/Nkx2.5) is identical to that of human (*17*, *22*). The Nkx2.5 homeodomain is 73% identical in sequence with the parent member of the NK-2 homeodomain family, the vnd (ventral nervous system defective)/NK-2 homeodomain of *Drosophila melanogaster*, first described by Kim and Nirenberg (*2*). All three proteins bind specifically to the same DNA sequence, 5′-CAAGTG-3′ (*4*, *5*). The NMR three-dimensional solution structure of the vnd/NK-2 homeodomain−DNA complex has been determined by Gruschus et al. (*23*) and shows that the homeodomain has a helix−turn−helix binding motif with recognition helix III inserted into the major groove of the specific duplex DNA and residues 47, 50, 51, and 54 making contact with specific DNA bases and with the N-terminal residues 3 and 5 making contacts with DNA bases in the adjacent minor groove. Thermodynamic parameters for thermally induced unfolding and DNA binding of wild-type NK-2 and mutants NK-2(H52R) and NK-2(H52R/T56W) have been reported by Gonzalez et al. (*7*).

A 79-residue segment which encompasses the homeodomain of Nkx2.5 (which has a full length of 318 amino acids) has been expressed while replacing the oxidizable cysteine residue with the isosteric serine at position 56 to produce Nkx2.5(C56S). The C56S substitution is not expected to influence DNA binding by Nkx2.5 because $Ser^{56}$ is at the opposite side of the helix III−DNA contact surface and the $\beta$-carbon of Ser is not <10 Å from bound DNA. The Nkx2.5(C56S) protein has been used in our studies after finding that the wild-type homeodomain containing $Cys^{56}$ is easily oxidized during purification. NMR results reported here indicate that the wild-type Nkx2.5 and mutant Nkx2.5(C56S) proteins have the same secondary structure and long-range contacts. For comparison, new NMR data on the secondary structure of free vnd/NK-2 in the presence of 500 mM NaCl are given. Information about the conformational stability of the Nkx2.5(C56S) homeodomain has been obtained from thermal unfolding/refolding studies. Thermodynamic parameters are reported for Nkx2.5(C56S) binding specific, 18 bp DNA at pH 7.4 in the presence of 100 mM NaCl and show the temperature dependence of DNA binding affinity as well as the enthalpic and entropic contributions from 10 to 37 °C.

## MATERIALS AND METHODS

*Chemicals.* The *Pfu* DNA polymerase and *Dpn*I restriction enzyme (Stratagene, La Jolla, CA), *Nco*I and *Bam*HI restriction enzymes (New England Biolabs, Beverly, MA), Luria-Bertani (LB) broth (KD Medical, Columbia, MD), EDTA-free protease inhibitor cocktail (Roche Applied Science, Indianapolis, IN), Enterokinase (Novagen, Madison, WI), and ampicillin, chloramphenicol, and isopropyl 1-thio-D-galactopyranoside (IPTG) (Sigma Chemical Co., St. Louis, MO) were of molecular biology grade. The high purity (fluorescence blank of ≤0.005%) of imidazole (Sigma Chemical Co.) was used to minimize the contents of oxidized derivatives that can be bound to protein during purification. Acetonitrile (Fisher Scientific), trifluoroacetic acid (Applied Biosystems), and water for HPLC were of HPLC grade. MES and MOPS (Sigma Chemical Co.) and other reagents were of analytical grade. Buffers used for calorimetry and spectroscopy measurements were either 20 mM MES at pH 6.0 (buffer A) or 20 mM MOPS at pH 7.4 (buffer B) with 0−100 mM NaCl and were prepared with distilled, deionized water filtered through a Millipore MilliQ-UV-Plus reagent grade system.

*Construction of the Recombinant Plasmid and Site-Directed Mutagenesis.* The 77-residue Nkx2.5 homeodomain was cloned into the pET-32a(+) Trx fusion vector (Novagen) with an N-terminal hexahistidine tag for affinity purification and a Trx tag for enhancing the solubility of the expressed protein. As a template in PCRs, the cDNA of full-length mouse Nkx2.5 in the vector pBluescript II SK (±), provided by Y. Kim (National Heart, Lung and Blood Institute, National Institutes of Health), was used. For the PCR amplification of the construct pET-32a(+) vector with the Nkx2.5 homeodomain, the following synthetic oligonucleotide primers were used: forward, 5′-GCC GAG ACG GCC ATG GCC GAG AGA CCA CGC GCA CGG-3′; and reverse, 5′-GGG CGG GGA TCC *TCA* CCC CAG AAG CTC CAG AGT CTG-3′. The forward primer introduced a restriction enzyme site for *Nco*I (underlined), the reverse primer for *Bam*HI (underlined), and the stop codon (italic). PCR was performed using *Pfu* DNA polymerase with the following cycling profile in a GeneAmp PCR system 2400 (Perkin-Elmer, Foster City, CA): initial denaturation at 95 °C for 2 min, 30 cycles of denaturation at 95 °C for 1 min, annealing at 50 °C for 1 min, and elongation at 72 °C for 1 min, and final extension at 72 °C for 10 min. The resulting construct, pET-32a(+)-Nkx2.5 HD, was verified by DNA sequencing.

To prevent the possibility of cysteine modification, we generated the C56S mutant protein by in vitro site-directed mutagenesis using the QuikChange II technique (Stratagene). The sequence of the forward mutagenic primer was 5′-C CGT CGC TAC AAG AGC AAG CGA CAG CG-3′, and the TGC codon for cysteine was changed to the AGC codon (underlined) for serine. The sequence of the reverse mu-

tagenic primer was 5′-CG CTG TCG CTT GCT CTT GTA GCG ACG G-3′, and the GCA anticodon for cysteine was changed to the GCT codon (underlined) for serine. PCR amplification was performed using *Pfu* DNA polymerase. Samples were subjected to twelve 30 s cycles of denaturation at 95 °C, followed by annealing for 1 min at 55 °C and elongation for 7 min at 68 °C. *Dpn*I restriction enzyme was used to digest the parental supercoiled double-stranded DNA. The constructed mutant plasmid was transformed into XL2-Blue ultracompetent *Escherichia coli* cells (Stratagene) for screening purposes. The plasmid DNA insert was sequenced to confirm the mutations.

*Protein Expression and Purification*. The C56S protein was overexpressed in BL21-CodonPlus(DE3)-RP *E. coli* cells (Stratagene) that contain extra copies of *argU*, and *proL* tRNA genes for performing high-level expression of recombinant proteins from GC-rich genomes and those of eukaryotic origin in *E. coli*. The bacterial cell culture with LB medium, containing 100 $\mu$g/mL ampicillin and 34 $\mu$g/mL chloramphenicol, was incubated in a shaker (PsycroTherm G-26, New Brunswick, Edison, NJ) at 225 rpm and 37 °C until the $OD_{600}$ reached 0.6−0.8. Expression was induced with 1 mM IPTG, and the cells were grown for an additional 3 h at 37 °C. The cells were harvested by centrifugation at 5000*g* for 10 min at 4 °C. The cell pellet from a 3 L culture was resuspended in 180 mL of lysis buffer [20 mM Tris-HCl (pH 8.0) and 500 mM NaCl with 5 mM imidazole and 0.2% Triton X-100 for reducing the level of nonspecific binding in Ni affinity chromatography], supplemented with an EDTA-free protease inhibitor cocktail (Sigma), nuclease, and lysozyme. The cell suspension was lysed by passing it through a French press (Thermo Spectronic, Rochester, NY) twice at 16 000 psi. The extract was clarified by ultracentrifugation in a Ti-45 rotor with an Optima L-100 XP ultracentrifuge (Beckman Coulter, Fullerton, CA) for 30 min at 40 000 rpm (93000*g*) at 4 °C. The supernatant was loaded onto a 5 mL Ni−NTA agarose column, and the column was washed with 30 mL (6 column volumes) of lysis buffer, followed by 30 mL aliquots of elution buffer [20 mM Tris-HCl (pH 8.0) and 500 mM NaCl with 5 to 300 mM stepwise increasing concentrations of imidazole]. Fractions were collected and analyzed for protein purity by 16% discontinuous SDS−polyacrylamide gel electrophoresis (Invitrogen, Carlsbad, CA). The fractions from 60 to 200 mM imidazole contained most of the homeodomain and were pooled and dialyzed against 20 mM Tris-HCl (pH 8.0) and 50 mM NaCl in the absence of imidazole for 6 h. To cut the His tag and Trx tag, approximately 20 units of enterokinase was added for each milligram of Nkx2.5(C56S) protein, and then the mixture was incubated overnight at room temperature. Two additional residues, alanine at the amino terminus and methionine in the penultimate position, derived from the pET-32a(+) vector after the protease cleavage step, are added to the sequence of Nkx2.5(C56S), resulting in a final length for the homeodomain protein of 79 residues (see Figure 1, below). The eluant after digestion with enterokinase was loaded again onto a 1 mL Ni−NTA agarose column for the purpose of separating the cleaved tags from the homeodomain. The flow-through fraction, containing most of the cut Nkx2.5(C56S) protein, was pooled and concentrated with an Amicon stirred ultrafiltration cell system (Millipore, Billerica, MA) with a 3 kDa cutoff YM3 membrane (Millipore). To remove impurities such as nucleic acid, reverse-phase chromatography was performed on a semi-preparative scale (5 $\mu$m particle, 300 Å, 1.0 cm × 25 cm) with a $C_4$ column (model 214TP1010, Vydac, Hesperia, CA) on an HPLC system (model HP1050, Hewlett-Packard, Waldbronn, Germany). The Nkx2.5(C56S) protein was eluted with an acetonitrile gradient from 35 to 40% in 0.1% (w/v) trifluoroacetic acid at a flow rate of 1 mL/min. The purity and homogeneity of Nkx2.5(C56S) were confirmed by a single band on SDS−PAGE and mass spectrometry giving a value of 9690.4 Da, in good agreement with the calculated molecular weight from the amino acid sequence of 9691.2. The purified proteins were dialyzed against water at 4 °C overnight and lyophilized in a freeze dryer. Before calorimetric and spectroscopic measurements, lyophilized proteins were redissolved in water, and a conventional salting out by 80% saturated ammonium sulfate on ice was performed to remove insoluble fractions and other particles that could contribute to light scattering. The precipitated proteins were resuspended and dialyzed against buffer A or B, and recentrifuged. A molar extinction coefficient at 280 nm (20 °C) of 9570 $M^{-1}$ $cm^{-1}$ for Nkx2.5(C56S) was calculated by the method of Perkins (*24*) and used for determining protein concentrations. Protein stocks (∼1 mg/mL) were stored on ice at 4 °C.

*Preparation of Duplex DNA for Calorimetric and Fluorescence Studies.* Single-stranded, 18-mer oligonucleotides, 5′-TGTGT**CAAGTG**GCTGTAG-3′ and its complement, 5′-CTACAGCCACTTGACACA-3′, containing the Nkx2.5 binding site, 5′-CAAGTG-3′, were synthesized and purified by The Midland Certified Reagent Co. (Midland, TX). Lyophilized single strands were dissolved in water, and duplex DNA was prepared by mixing equal molar amounts of the complementary single strands in the presence of 80 mM NaCl at 25 °C. Annealing was achieved by placing a microfuge tube containing the oligonucleotide mixture in a 1 L water bath at 85 °C for 5 min, and then slowly cooling the water bath with the sample by moving the bath first to the benchtop until it reached room temperature and second to a refrigerator at 4 °C. Using 20% polyacrylamide−TBE gels (Novex, Invitrogen Co.) for gel electrophoresis and visualization with either SYBR Green II (Molecular Probes, Eugene, OR) or silver staining (SilverXpress Kit, Invitrogen Co.), only a single band corresponding to duplex DNA ($M_r$ = 11 000) in the DNA stock solution was detected after annealing. Stock solutions of 18 bp DNA (∼0.5 mM) were stored on ice at 4 °C.

A molar extinction coefficient of 254 000 $M^{-1}$ $cm^{-1}$ at 260 nm for the 18 bp, duplex DNA was determined using a pragmatic approach. Since we knew there was 1:1 binding between the homeodomain and the specific 18 bp DNA and also the exact concentration of Nkx2.5(C56S), we could solve for the correct duplex DNA extinction coefficient by using the fitting procedure (see below) for each of 14 different ITC titrations to give a stoichiometry of unity. This procedure was possible because the protein was stable and the absorbance of the DNA in the ITC cell had been measured before each experiment in which protein had been injected into the DNA solution. The magnitude of the hyperchromic effect (22%) was determined by heating a sample of the 18 bp duplex DNA at 60 °C/h from 15 to 75 °C and monitoring the absorbance changes at 260 nm, and then extrapolating

the absorbance change to 20 °C. A value of 346 200 ± 10% $M^{-1}$ $cm^{-1}$ was calculated (*25*) for the two complementary strands from the sequences of bases and near-neighbor effects (communicated by H. Klump), which after correcting for the hyperchromic effect gave a value 1.06 greater than that estimated by us. Using just the extinction coefficients of free bases at 260 nm gave an overestimate of ~20%.

*NMR Methods*. The NMR samples consisted of 2 mM $^{15}$N-labeled NK-2 homeodomain in 500 mM NaCl and of 1 mM wild-type or C56S mutant Nkx2.5 homeodomain, in both the unbound state and bound to the NK-2 consensus DNA (16-mer duplex) in 80 or 500 mM NaCl and 20 mM $NaPO_4$ (*26*). All protein samples were at pH ~7. A sample using a DNA-bound, longer wild-type Nkx2.5 homeodomain construct [from Lee et al. (*27*)], which includes the NK-2-specific domain, also was analyzed. Spectra for the DNA-bound NK-2 and for unbound wild-type Nkx2.5 were recorded on a Bruker 600 MHz DRX spectrometer, and for the C56S mutant samples, a Bruker 800 MHz Avance spectrometer was used. One-dimensional (1D) spectra and two-dimensional (2D) $^{15}$N HSQC spectra were collected for the unbound samples from 12 to 55 °C. Three-dimensional (3D) $^{15}$N NOESY HSQC spectra (*28*) were collected for the unbound samples at 25 °C for NK-2, and at 12 and 27 °C for the Nkx2.5 samples. 2D $^{15}$N HSQC and 3D $^{15}$N NOESY HSQC spectra were collected at 35 °C for the DNA-bound samples. All spectra were processed with nmrPipe (*29*).

*Sample Preparation for Calorimetry and Spectroscopy Studies*. Slide-A-Lyzer cassettes (3500 MW cutoff; Pierce) were used to dialyze Nkx2.5(C56S) (~1 mg/mL) and 18 bp DNA (~5.5 mg/mL) against two 1 L portions of the indicated buffer at 4 °C for ~24 h. For Nkx2.5 binding 18 bp DNA in ITC experiments, the protein and DNA were placed in separate cassettes and suspended in the same buffer (buffer B with 100 mM NaCl) for dialysis. At the end of dialysis (just before experiments), protein and DNA samples were diluted with the final dialysate and centrifuged, and UV spectra were measured at 20 °C in a diode array Hewlett-Packard 8453 spectrophotometer equipped with a Peltier temperature control device. The absorbance of protein samples at 340 nm ($A_{340}$) was used to correct the $A_{280}$ for light scattering (observed $A_{280} - 2.174A_{340} =$ corrected $A_{280}$) for calculating Nkx2.5(C56S) concentrations. Just prior to the ITC cell being loaded, the duplex 18 bp DNA stock was diluted to ~1 $\mu$M and the absorbance at 260 nm determined for calculation of the DNA concentration for each titration. In all experiments, the final dialysate was used as a reference buffer.

*Circular Dichroism*. Far-UV circular dichroism (CD) measurements were performed using a Jasco-710 spectropolarimeter equipped with a Neslab RT-110 (Thermo NESLAB, Inc., Newington, NH) computer-controlled, water-circulating bath-type thermostat. Typically, 0.2−0.5 mg/mL Nkx2.5-(C56S) homeodomain concentrations in buffers A and B with 0−100 mM NaCl were measured using a jacketed cylindrical quartz cell with a light path length of 0.050 cm. CD spectra of the protein were recorded between 195 and 260 nm and were corrected for the buffer CD signal. The data were expressed in mean residue molar ellipticity units (degrees square centimeter per decimole) where the mean residue molecular weight is 122.45 for Nkx2.5(C56S). CD spectra were analyzed for secondary structure composition using the convex constraint algorithm (CCA) of Perczel et al. (*30*). Thermal unfolding of the protein was monitored by recording the ellipticity value at 222 nm while increasing the temperature of the sample from 10 to 80 °C at a rate of 60 °C/h. Progress ellipticity curves were analyzed by a two-state equilibrium model using the EXAM program of Kirchhoff (*31*).

*Differential Scanning Calorimetry*. DSC measurements were performed using a VP-DSC calorimeter (*32*) with a sample cell volume of 0.5114 mL, from MicroCal, LLC (Northampton, MA). The instrument baseline was determined before each sample scan, by filling both the reference and sample cells with the same buffer dialysate that contained the sample, and using the same scanning parameters. Nkx2.5-(C56S) homeodomain, from 0.12 to 0.95 mg/mL in buffer A or B with or without NaCl, was scanned from 10 to 80 °C, at a rate of 60 °C/h, without feedback. Before the start and between repeated heating cycles, samples were allowed to equilibrate for 1 h at 10 °C before heating. At the end of a scan, samples were cooled immediately to the starting temperature. Heat capacity data were corrected for the instrument baseline, normalized for scan rate and protein concentration, and expressed in kilocalories per kelvin per mole (1.000 cal = 4.184 J). Excess heat capacity profiles were analyzed by a two-state equilibrium model using the EXAM program of Kirchhoff (*31*) as previously described (*33*). The enthalpy ($\Delta H_T$), free energy ($\Delta G_T$), and entropy ($\Delta S_T$) of unfolding at 298 K were calculated as follows:

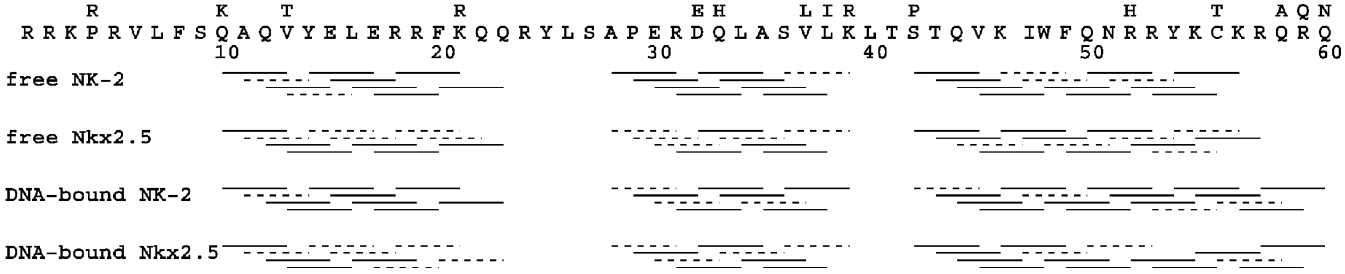


FIGURE 1: Sequence and helix lengths of free and DNA-bound NK-2 and Nkx2.5 homeodomains. The sequence of the Nkx2.5 homeodomain is indicated with those residues that are different in NK-2 shown above. Lines representing the αN $i-i+3$ cross-peaks from 3D $^{15}$N NOESY spectra for free and DNA-bound NK-2 and Nkx2.5 homeodomains are shown. These signals indicate the helical regions of the proteins. Dashed lines indicate αN $i-i+3$ signals which are ambiguous, typically due to degeneracy with intraresidue or sequential αN signals. The actual Nkx2.5 protein used in our studies has 10 additional amino acids at the N-terminus ($NH_2$-AMAERPRARR) and 9 additional residues at the C-terminus (QDQTLELLG-COOH). Both DNA-bound NK-2 and Nkx2.5 proteins are complexed to the same 16 bp DNA containing the target site (5′-CAAGTG-3′) in the core.

$$\Delta H_T = \Delta H_{T_m} - \Delta C_p(T_m - T)$$

$$\Delta G_T = (1 - T/T_m)\Delta H_{T_m} - (T_m - T)\Delta C_p + T\Delta C_p \ln(T_m/T)$$

$$\Delta S_T = {T_m}^{-1}\Delta H_{T_m} - \Delta C_p \ln(T_m/T)$$

where $T_m$ and $\Delta H_{T_m}$ are the unfolding midpoint temperature and the van't Hoff enthalpy of unfolding, respectively, and $\Delta C_p$ is the heat capacity change of unfolding calculated from the plot of van't Hoff enthalpies at different NaCl concentrations versus the midpoint temperatures.

*Isothermal Titration Calorimetry*. Binding studies were performed from 10 to 37 °C, in buffer B with 100 mM NaCl, using a VP-ITC titration calorimeter (MicroCal, LLC) with a reaction cell volume of 1.4061 mL. Typically, 0.7−1.0 $\mu$M specific, 18 bp duplex DNA in the reaction cell was titrated with a 18−23 $\mu$M solution of Nkx2.5(C56S) homeodomain contained in a 250 $\mu$L syringe. At least 30−35 consecutive injections of 5 $\mu$L at 2 s/$\mu$L were applied at 6 min intervals while the DNA solution was stirred at a constant speed of 300 rpm. Protein heats of dilution were calculated from the average heats of the last 10−15 injections, and these values were subtracted from the measured heats of binding. Binding enthalpies were calculated from the average second through eighth or twelfth injections while the DNA was in molar excess of the protein. Titration curves were analyzed with Origin, provided with the instrument by MicroCal LLC, using a one-site binding model to fit the curves. The free energy ($\Delta G_T$) and entropy of binding ($T\Delta S_T$) at 298 K were calculated according to the relations $\Delta G_T = -RT \ln K_T$ and $T\Delta S_T = \Delta H_T + RT \ln K_T$, where R is the universal gas constant (1.987 cal $K^{-1}$ $mol^{-1}$) and $K_T$ is the binding constant at 25 °C.

*Fluorescence Spectroscopy*. Steady-state fluorescence emission spectra were recorded using a QM-6SE (PTI, London, ON) spectrofluorometer without polarizers, equipped with a temperature-controlled sample holder. Measurements were performed using a path length of 3 mm and 150 $\mu$L quartz cells. Excitation at 295 nm was used with bandwidths of 1 and 4 nm in the excitation and emission paths, respectively. Protein fluorescence spectra were corrected for the corresponding background signal of the buffer, buffer with urea, or buffer with DNA. When DNA was present, the fluorescence emission intensities were further corrected for the inner filter effects.

## RESULTS

*NMR Structure of the Nkx2.5 Homeodomain*. The vnd/NK-2 and wild-type and C56S Nkx2.5 homeodomains exhibit nearly identical secondary structure (data summarized in Figure 1) and very similar long-range contacts between the conserved residues of the hydrophobic core (data not shown), indicating similar three-dimensional structures. A previous report on the secondary structure of NK-2 without added salt showed a shorter third helix, extending to residue 53 in a spectrum measured at 12 °C (*26*). The addition of 500 mM NaCl to NK-2 stabilizes the homeodomain, increasing the unfolding transition temperature to ~52 °C (*7*) and extending the third helix to residue 57 at 25 °C. The third helix of Nkx2.5 is slightly longer, at both 80 and 500 mM NaCl, extending to residue 58. The unbound, wild-type Nkx2.5 unfolding transition monitored by NMR starts to occur at temperatures greater than 35 °C, with the C56S mutant exhibiting similar behavior. In the DNA-bound forms of NK-2 and Nkx2.5, the third helix extends further, to residue 61 in both cases. For DNA-bound NK-2, the data in Figure 1 are from the NMR spectra used to determine the structure (*23*). The residues contacting DNA in the DNA-bound Nkx2.5 show large chemical shift changes compared to the unbound HD samples (*27*), and the changes were very similar to those observed for the NK-2−DNA complex compared to free NK-2 (*23*). Despite the lower concentration of the DNA-bound Nkx2.5 sample, two of the strongest protein−DNA NOE signals are still observed in the 3D spectra (between N51 and the DNA major groove and between R5 and the DNA minor groove), indicating that both the wild type and C56S mutant of Nkx2.5 bind DNA in the same manner as the NK-2 HD.

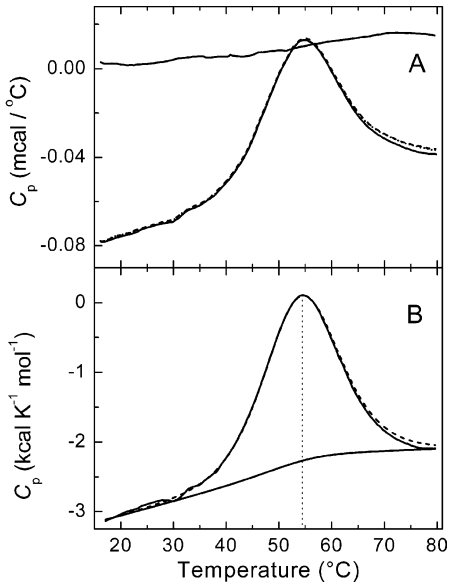


FIGURE 2: Representative DSC profile of the Nkx2.5(C56S) homeodomain. Heat capacity profiles of 0.49 mg/mL protein in 20 mM MOPS/100 mM NaCl (pH 7.4) buffer were recorded at a scan rate of 60 °C/h. (A) Three consecutive heating cycles with rapid cooling between the scans and a 60 min equilibration at the start temperature (first, second, and third scans as solid, dashed, and dotted curves, respectively) are shown with the instrument baseline (solid line on the top). (B) Experimental data of the first heating scan (solid line) and the fit by a two-state equilibrium model (dashed line).

*Conformational Stability of the Nkx2.5(C56S) HD.* Thermal unfolding of the Nkx2.5(C56S) homeodomain has been studied by DSC and far-UV CD.

A representative DSC experiment with 0.5 mg/mL Nkx2.5-(C56S) homeodomain at pH 7.4 in buffer B with 100 mM NaCl is shown in Figure 2. The instrument baseline and the raw calorimetric data of three consecutive heating scans are shown (Figure 2A). The excess heat capacity profiles of the protein corresponding to the first, second, and third scans show no significant difference in areas or shapes of endotherms. This indicates that the thermally induced unfolding can be repeated. Also, post-transitional baselines do not show any sign of protein aggregation at high temperatures (to 80 °C). After correction for the instrument baseline and

Table 1: Thermodynamic Parameters for Unfolding of Nkx2.5(C56S) Obtained from DSC and CD Experiments under Different Conditions[a]

| buffer | [NaCl] (mM) | method | $T_m$ (°C) | $\Delta H_{cal}$ (kcal/mol) | $\Delta H_{vH}$ (kcal/mol) | $\Delta H_{cal}/\Delta H_{vH}$ |
|---|---|---|---|---|---|---|
| MES (pH 6.0) | − | DSC | 45.6 | 34 | 34 | 1.0 |
| | | CD | 45.8 | | 34 | |
| | 100 | DSC | 53.7 | 44 | 44 | 1.0 |
| | | CD | 53.3 | | 49 | |
| MOPS (pH 7.4) | − | DSC | 44.4 | 34 | 34 | 1.0 |
| | | CD | 44.1 | | 34 | |
| | 25 | DSC | 49.9 | 41 | 41 | 1.0 |
| | 50 | DSC | 52.3 | 42 | 43 | 0.9 |
| | | CD | 52.0 | | 40 | |
| | 100 | DSC | 54.4 | 44 | 45 | 0.9 |
| | | CD | 53.9 | | 44 | |

[a] For each experiment, the transition midpoint temperature ($T_m \pm 0.2$ °C), calorimetric enthalpy ($\Delta H_{cal} \pm 5\%$), and van't Hoff enthalpy ($\Delta H_{vH}$) were obtained by fitting DSC and CD data to a two-state, equilibrium model for unfolding.

normalization for the scan rate and protein concentration, the heat capacity data could be fit to a two-state equilibrium transition model (Figure 2B). This model gives values of 45 ± 3 kcal/mol for the van't Hoff enthalpy of unfolding and 54.4 ± 0.2 °C for the transition midpoint temperature. The cooperativity ratio, obtained as the ratio of the calorimetric to the van't Hoff enthalpies, is 0.99, which further indicates that the Nkx2.5(C56S) homeodomain unfolds as a single cooperative unit, with no stable intermediates present during the unfolding process.

The thermal unfolding of the Nkx2.5(C56S) homeodomain is repeatable and follows a two-state unfolding model in both 20 mM MES (pH 6.0) and 20 mM MOPS (pH 7.4) buffers, either in the absence or in the presence of NaCl. The thermodynamic parameters obtained from the two-state analysis of the DSC profiles of the homeodomain under these different conditions are given in Table 1. The transition midpoint temperatures as well as calorimetric and van't Hoff enthalpies of unfolding do not differ significantly at different pH values at the same NaCl concentrations.

Far-UV CD spectra of Nkx2.5(C56S) in buffer B with 100 mM NaCl are shown in Figure 3A. At 15 °C when the homeodomain is folded, an α-helical content of 51% is estimated from the convex constraint algorithm for prediction of secondary structure from far-UV spectra (*30*). This value agrees well with NMR data which indicate that 53% of the residues are in an α-helical conformation (Figure 1). The secondary structure of the Nkx2.5(C56S) homeodomain is disrupted by heating, but its folded conformation is fully regained after cooling (Figure 3A). A second heating from 15 to 80 °C followed by cooling results in an identical spectrum at 15 °C. These observations indicate that the thermal unfolding of Nkx2.5(C56S) is fully reversible. Similar results have been obtained for this homeodomain in different buffers (Table 1). The high-temperature far-UV CD spectrum is the same at either 80 or 91 °C, and suggests that some residual $\beta$-loop structures or tertiary interactions are not thermally labile. Actually, the ellipticity at 222 nm for Nkx2.5(C56S) in 8 M urea is 30% of that at 80 °C, confirming that the HD has some residual structure at high temperatures. The far-UV CD spectra for Nkx2.5(C56S) at low and high temperatures are remarkably similar to those reported by Damante et al. (*8*) for thyroid transcription factor 1 (TTF-1).

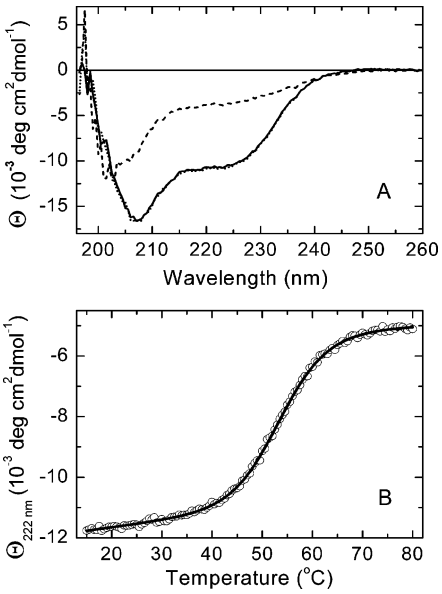


FIGURE 3: Representative CD data of the Nkx2.5(C56S) homeodomain. (A) Far-UV CD spectra for 0.49 mg/mL Nkx2.5(C56S) in the same buffer as in Figure 2, recorded at 15 °C: before heating (solid line), at 80 °C after the first heating at 60 °C/h (dashed line), and at 15 °C after cooling (dotted line). (B) Mean residue molar ellipticity changes at 222 nm as a function of increasing temperature (60 °C/h). Experimental data from the first heating (○) and the fit to a two-state equilibrium model (solid line) are shown.

A progress curve for the ellipticity changes at 222 nm as a function of increasing temperature for Nkx2.5(C56S) at pH 7.4 is shown in Figure 3B. As many as four repeated heating and cooling cycles at a rate of 60 °C/h have been performed from 15 to 80 °C (data not shown), and the CD progress curves overlap, which indicates that the unfolding−folding processes are reversible. Progress curves could be fit well to a two-state unfolding model (Figure 3B, solid curve). The unfolding midpoint temperature and van't Hoff enthalpy of unfolding obtained from the two-state fit under these conditions are 54 °C and 44 kcal/mol, respectively. These values are in excellent agreement with the unfolding parameters obtained by DSC. Similar experiments have been performed using different buffer conditions, and the data obtained from the two-state fits of the progress ellipticity curves agree well with those obtained by DSC (Table 1).

The stabilization of Nkx2.5(C56S) in buffer B at pH 7.4 by NaCl is illustrated in Figure 4. In all cases, the excess heat capacity profiles are well fit by a thermodynamic two-state unfolding model (Figure 4A). Over the limited concentration range of 0−100 mM NaCl, the plot of $\Delta H_{vH}$ values versus midpoint temperatures of unfolding ($T_m$) from DSC (Figure 4A) is linear (Figure 4B). The slope of the plot in Figure 4B gives a value for the heat capacity change during unfolding of Nkx2.5(C56S) of 1.2 ± 0.1 kcal $K^{-1}$ $mol^{-1}$, which is ∼2-fold greater than that measured for NK-2 unfolding (*7*). For the Nkx2.5(C56S) homeodomain with 200 mM NaCl, the transition temperature is further increased but the unfolding process is not a two-state process (data not shown).

Estimated values of $\Delta C_p$ from the two-state analyses of DSC data (Figure 2B) are only ∼11% of the value given by NaCl stabilization (Figure 4). This is because the pretransition excess heat capacity of the DSC data for the homeodomain has a considerable slope (Figure 2). As discussed by Privalov

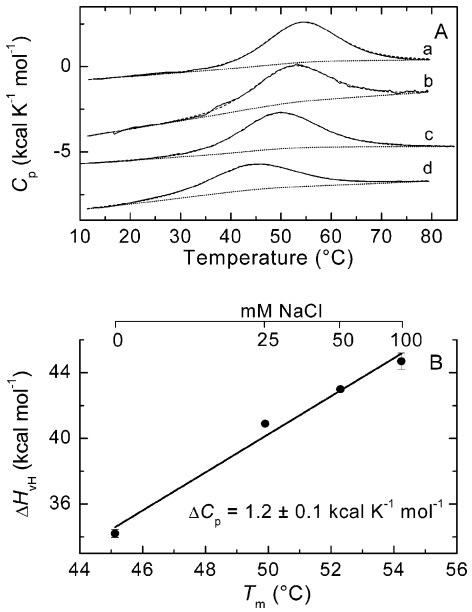


FIGURE 4: Stabilization of Nkx2.5(C56S) by increasing NaCl concentrations in 20 mM MOPS (pH 7.4) buffer. (A) DSC profiles in the absence (d) and presence of 25 (c), 50 (b), and 100 mM NaCl (a), after subtraction of the instrument baselines and normalization for scan rate and protein concentrations. The baselines generated by the EXAM program and the two-state fits (dashed lines) are shown. (B) Plot of the van't Hoff enthalpies of unfolding at different NaCl concentrations (●) vs the transition midpoint temperatures. The slope of the linear least-squares fit (solid line) of the data gives a heat capacity change for unfolding of 1.2 ± 0.1 kcal $K^{-1}$ $mol^{-1}$.

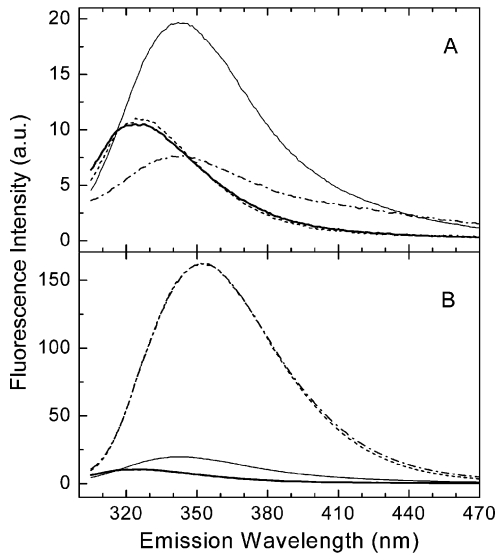


FIGURE 5: Tryptophan fluorescence emission spectra of Nkx2.5-(C56S) and NK-2 homeodomains. Emission spectra of proteins (0.15 mg/mL) in 20 mM MOPS/100 mM NaCl (pH 7.4) buffer were recorded at 25 °C with excitation at 295 nm; intensities are expressed in arbitrary units. (A) Comparison of the free and 18 bp specific DNA-bound proteins: free Nkx2.5(C56S) (thick solid line), Nkx2.5(C56S)/DNA mixture (1:1.25 molar ratio) (dashed line), free NK-2 (thin solid line), and NK-2/DNA mixture (1:1.05 molar ratio) (dashed−dotted line). (B) Enhancement of the Trp fluorescence emission of the homeodomains upon denaturation by 8 M urea. Spectra of Nkx2.5(C56S) (thick solid line) and NK-2 (thin solid line) are the same as in panel A. Spectra of denatured Nkx2.5-(C56S) and NK-2 are represented by dashed and dashed−dotted lines, respectively. Protein fluorescence spectra are corrected as described in Materials and Methods.

(*34*), fluctuations of the native structure in nonrigid proteins can accumulate significant thermal energy with an increasing temperature. Nevertheless, the baseline for the endotherm shown in Figure 2B is approximately correct because ITC titrations of specific DNA with Nkx2.5(C56S) indicate that the homeodomain is folded up to 37 °C, and only at >40 °C do we see evidence of homeodomain unfolding (data not shown).

*Tryptophan Fluorescence.* Nkx2.5(C56S) and the *Drosophila* vnd/NK-2 homeodomains have a single Trp residue at position 48 within helix III of the homeodomain. $Trp^{48}$ is conserved among the DNA recognition helices of all common homeodomains. An unusually low quantum yield of the conserved $Trp^{48}$ in the native state and large intensity increases upon unfolding in denaturants (urea or guanidine) have been reported for several other homeodomains [see the paper of Nanda and Brand (*35*)].

Initial measurements of the Trp fluorescence of Nkx2.5-(C56S) indicated that this differed significantly from earlier observations made with the vnd/NK-2 homeodomain (M. Gonzalez and A. Ginsburg, unpublished data). Accordingly, we have directly compared the Trp emission spectra of Nkx2.5(C56S) and vnd/NK-2 homeodomains (using the same buffer, temperature, and excitation at 295 nm) in the absence and presence of a molar excess of specific 18 bp DNA or 8 M urea (Figure 5). Although the NMR structures of these two homeodomains bound to specific duplex DNA are alike, the unbound homeodomains Nkx2.5 and vnd/NK-2 have different Trp flourescence emission spectra at 25 °C (Figure 5A). Emission maxima of quenched $Trp^{48}$ in homeodomains are 325 nm for Nkx2.5(C56S) and 342 nm for vnd/NK-2. The integrated area of the emission spectrum for vnd/NK-2 is 2.4 times that for Nkx2.5(C56S). A further quenching of $Trp^{48}$ fluorescence occurs when the homeodomain vnd/NK-2 forms a complex with specific 18 bp DNA. Fluorescence decreases upon binding DNA are 0% for Nkx2.5(C56S) and 49% for vnd/NK-2 (without shifting the emission peak), as measured by relative emission peak areas corrected for inner filter effects. Experiments conducted at 20 °C (rather than at 25 °C) showed that the level of quenching of Trp fluorescence of the vnd/NK-2 homeodomain produced by DNA binding is 16% lower, which suggests that dynamic quenching is involved (i.e., a collision-mediated type of quenching). Unfolding of the homeodomains in 8 M urea produces red shifts to 353 nm of emission peaks and gives the same emission spectrum (Figure 5B). Emission peak areas of the native homeodomains are proportional to the quantum yields of $Trp^{48}$ and, upon unfolding in 8 M urea, increase 18-fold for Nkx2.5 and 7.7-fold for vnd/NK-2.

*Thermodynamics of Nkx2.5 Binding Sequence-Specific DNA.* Binding of Nkx2.5(C56S) to specific 18 bp DNA has been measured in 20 mM MOPS/100 mM NaCl buffer at pH 7.4. A representative ITC experiment at 20 °C, in which 0.80 $\mu$M 18 bp DNA has been titrated with 21.62 $\mu$M Nkx2.5(C56S) homeodomain, is shown in Figure 6. Under these conditions, the differential heats (top panel) produced by injections of 5 $\mu$L of protein into the DNA solution are constant through the second and tenth injections, and these values were averaged to give a precise value for the enthalpy of binding DNA at saturating DNA concentrations. After the tenth injection of protein, the observed heats of binding begin to decrease as the free DNA is being depleted, and a constant

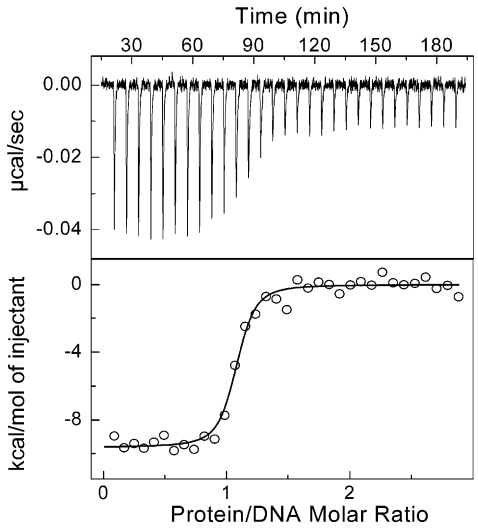


FIGURE 6: Representative isothermal titration of the specific 18 bp DNA with Nkx2.5(C56S) in 20 mM MOPS and 100 mM NaCl at pH 7.4 and 20 °C. The sample cell contains 0.80 $\mu$M DNA, and the syringe contains 21.62 $\mu$M protein. The top panel presents the observed heats of binding for the second through 35th injections of 5 $\mu$L of protein solution into DNA at 6 min intervals after baseline subtraction. The bottom panel shows the binding enthalpies (○) obtained after subtraction of the average heat of dilution of the HD from the individual integrated heats, and normalization for protein concentration. Data are fit to a one-site binding model (solid curve).

heat of addition is reached after the nineteenth injection when all of the DNA has been bound by the homeodomain. Further additions of protein represent the heat of dilution of the protein, which is approximately the same as that obtained by adding protein to buffer. The average of these values (the last 16 additions) was used to correct the observed enthalpies of binding. The fit of the titration curve produced by the corrected enthalpies versus the total homeodomain protein to DNA molar ratio (bottom panel, Figure 6) to a model with a single class of binding sites with a stoichiometry for binding of 1 (see Materials and Methods) yields a binding enthalpy $\Delta H$ of $-9.6 \pm 0.2$ kcal/mol, and an association constant $K_A'$ of $(2.4 \pm 0.6) \times 10^8$ M$^{-1}$ at 20 °C.

Titrations were performed at different temperatures from 10 to 37 °C. In this temperature range, both the protein (Figure 2; $T_m = 54$ °C) and the 18 bp duplex DNA (DSC $T_m = 72$ °C) are in native, fully folded states. The average association constants and average binding enthalpies of one to three separate experiments are summarized in Table 2. In each case, the apparent association constant, $K_A'$, is on the order of magnitude of $10^8$ M$^{-1}$, which reflects a high-affinity binding of the homeodomain to the specific 18 bp duplex DNA. From 10 to 37 °C, there is a small increase in association constant values. Values of the enthalpies for Nkx2.5(C56S) binding specific DNA decrease from $-7.3$ to $-12.4 \pm 0.3$ kcal/mol over the temperature range of 10−37 °C (Table 2).

Thermodynamic parameters for Nkx2.5(C56S) homeodomain binding sequence-specific 18 bp DNA as function of temperature are shown in Figure 7. The plot of the binding enthalpies versus temperature (Figure 7) are fitted by a straight line in the temperature range that was studied (10−37 °C). The negative slope of this plot gives a heat capacity change of $-0.18 \pm 0.01$ kcal K$^{-1}$ mol$^{-1}$ for Nkx2.5(C56S)

Table 2: Apparent Affinity Constant ($K_A'$) and Apparent Enthalpy of Binding ($\Delta H$) for Nkx2.5(C56S) Homeodomain Binding Sequence-Specific, 18 bp DNA in 20 mM MOPS and 100 mM NaCl at pH 7.4 and Different Temperatures[a]

| temp (°C) | $K_A'$ ($\times 10^{-8}$ M$^{-1}$) | $\Delta H$ (kcal/mol) |
|---|---|---|
| 10 | $2.5 \pm 1.0$ (2) | $-7.3 \pm 0.3$ (17) |
| 15 | $1.2 \pm 0.2$ (1) | $-8.6 \pm 0.1$ (6) |
| 20 | $2.5 \pm 0.9$ (3) | $-9.7 \pm 0.1$ (27) |
| 23 | $5.9 \pm 1.8$ (1) | $-9.8 \pm 0.1$ (12) |
| 25 | $4.9 \pm 2.0$ (2) | $-10.3 \pm 0.6$ (18) |
| 30 | $4.9 \pm 1.0$ (2) | $-11.4 \pm 0.2$ (20) |
| 33 | $4.2 \pm 1.6$ (1) | $-11.8 \pm 0.2$ (9) |
| 35 | $5.4 \pm 1.4$ (1) | $-12.0 \pm 0.1$ (11) |
| 37 | $6.0 \pm 1.5$ (1) | $-12.4 \pm 0.1$ (10) |

[a] The binding parameters were obtained by fitting the ITC data to a one-site binding model. The stoichiometry of binding is 1.0 in each experiment (see Materials and Methods). For $K_A'$ values at each temperature, one to three titrations are indicated in parentheses. The errors given for a single titration are the errors of the fit, and for more than one titration, errors are the standard deviations from the mean. The total number of values obtained at a saturating DNA concentration that were used for calculating the apparent enthalpy of binding is indicated in parentheses with $\Delta H$ values.

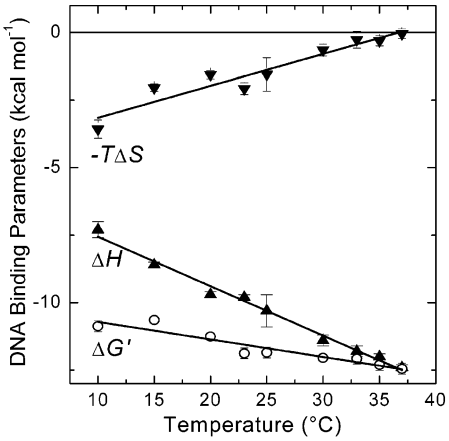


FIGURE 7: Thermodynamic parameters for Nkx2.5(C56S) binding sequence-specific 18 bp DNA as a function of temperature. Enthalpies [$\Delta H$ (▲)], entropies [$-T\Delta S$ (▼)], and Gibbs free energies of binding [$\Delta G'$ (○)] vs temperature and the corresponding linear regressions of the data (solid lines) are presented. Error bars represent the standard deviations of one to three experiments (see Table 2) and are within the symbol size for $\Delta G'$ values. The slope of the linear least-squares fit of the binding enthalpies gives a heat capacity change for binding $\Delta C_p$ of $-0.18 \pm 0.01$ kcal K$^{-1}$ mol$^{-1}$.

binding specific 18 bp DNA. The binding of DNA is enthalpically controlled at all temperatures. At lower temperatures, there is a small positive entropy contribution to the binding, which approaches zero as the temperature reaches 37 °C. Values for the apparent free energy of binding DNA decrease from $-10.9$ to $-12.5$ kcal/mol as the temperature increases from 10 to 37 °C.

The standard thermodynamic parameters at pH 7.4 and 298 K for Nkx2.5(C56S) unfolding and for vnd/NK-2 and the mutant NK-2(H52R) unfolding from the studies of Gonzalez et al. (*7*) are summarized in Table 3. Values of $\Delta C_p$ used for temperature extrapolations (see Materials and Methods) also are given in Table 3. Thermodynamic parameters for Nkx2.5(C56S) and, for comparison, vnd/NK-2, NK-2(H52R), and NK-2(H52R/T56W) binding sequence-specific, duplex DNA at pH 7.4 and 298 K are given in Table 4 (see below). Large errors are associated with the calculated thermodynamic parameters for protein unfolding due to long

Table 3: Thermodynamic Parameters at pH 7.4 and 298 K from Thermal Unfolding Studies of Nkx2.5(C56S), NK-2, and NK-2(H52R) Homeodomains[a]

| protein | $T_m$ (°C) | $\Delta H$ (kcal/mol) | $\Delta G'$ (kcal/mol) | $-T\Delta S$ (kcal/mol) | $\Delta C_p$ (kcal $K^{-1}$ $mol^{-1}$) |
|---|---|---|---|---|---|
| Nkx2.5(C56S) | 54.2 | $10 \pm 2.9$ | $2.4 \pm 4.0$ | $-7.6 \pm 2.8$ | $1.2 \pm 0.1$ |
| NK-2 | 43.0 | $8.8 \pm 5.6$ | $1.2 \pm 7.5$ | $-7.6 \pm 5.4$ | $1.4 \pm 0.3$ |
| NK-2(H52R) | 51.2 | $13.3 \pm 8.1$ | $2.4 \pm 10.9$ | $-10.9 \pm 7.8$ | $1.3 \pm 0.3$[b] |

[a] Parameters and their errors are calculated on the basis of the equations specified in Materials and Methods. The errors originate from the standard deviations in $\Delta C_p$ (Figure 4) and $\Delta H_{vH}$ (Table 1), assuming no error in $T_m$. For Nkx2.5(C56S), $T_m$ and $\Delta H_{vH}$ have been obtained by DSC in 20 mM MOPS and 100 mM NaCl (pH 7.4), whereas for NK-2 and NK-2(H52R), values are from the CD results of Gonzalez et al. (*7*) in 50 mM Hepes and 100 mM NaCl (pH 7.4). [b] From CD measurements in the absence and presence of 100 mM NaCl (*7*), assuming the same error that was found for wild-type NK-2.

temperature extrapolations from observed $T_m$ values, whereas errors are much smaller for the homeodomains binding specific 18 bp DNA at 298 K since the binding measurements encompass the range of 10−25 °C for the vnd/NK-2 proteins (*7*) and 10−37 °C for Nkx2.5(C56S). There are important differences between Nkx2.5 and the NK-2 proteins in the thermodynamics of specific DNA binding, as will be discussed below.

## DISCUSSION

The Csx/Nkx2.5(C56S) homeodomain undergoes reversible, thermally induced two-state unfolding as measured by either DSC or far-UV CD changes. In contrast, vnd/NK-2 and the mutant NK-2(H52R) show non-two-state unfolding in DSC but two-state unfolding in far-UV CD measurements (*7*). Using the latter values, the thermodynamic parameters calculated for the standard state of pH 7.4 and 298 K can be compared to those calculated for Nkx2.5(C56S) unfolding (Table 3). However, there are large errors associated with the thermodynamic parameters due to the extrapolations from $T_m$ values to 298 K and the errors in $\Delta C_p$ values, which are known with certainty for only Nkx2.5(C56S) and NK-2. Values of $\Delta C_p$ have been obtained from the stabilization of these homeodomains by added NaCl. Values of $\Delta C_p$ could not be obtained directly from DSC data because fluctuations in native structures at low temperatures give a large pretransitional slope (*34*) that obscures the heat capacity change for unfolding; see Figure 2. Flexibility is thought to be an important feature of homeodomains for recognition and binding to specific DNA sequences in long stretches of DNA (*8*, *36*).

The Nkx2.5(C56S) HD has a greater thermal stability than vnd/NK-2, and this can be attributed to an additional ion pair interaction between the side chains of $Arg^{52}$ and $Glu^{17}$ as in the case of NK-2(H52R) (*10*, *23*). The NK-2(H52R) mutant has a transition temperature for unfolding similar to that of Nkx2.5(C56S) (Table 3). All three homeodomains contain an ion pair interaction between conserved residues $Arg^{19}$ and $Glu^{30}$ (*23*). Fluorescence studies indicate that the conserved $Trp^{48}$ of vnd/NK-2 is less quenched than that of Nkx2.5(C56S) and can be dynamically quenched to approximately the same degree as observed for unbound Nkx2.5(C56S) by binding specific DNA, which stabilizes the tertiary structure of vnd/NK-2. This indicates that the unbound vnd/NK-2 HD has a more flexible structure than Nkx2.5, and this is possibly why non-two-state unfolding of vnd/NK-2 has been observed in earlier DSC studies (*7*). The difference between Trp fluorescence emission spectra of Nkx2.5(C56S) and vnd/NK-2 is probably due to the His residue at position 52, which is 5 Å from $Trp^{48}$ in NK-2. Note that Y54 is too far from W48 (13 Å) to be a factor.

The importance of aromatic residues in the hydrophobic core of homeodomains is illustrated by the findings of Subramaniam et al. (*9*), who showed that W48F and F8A mutants of the Bcd-HD are destabilized relative to the wild-type Bcd-HD and have lost their ability to bind specific DNA. These workers hypothesize that the aromatic residues at positions 8 and 48 are factors in coordinating the orientation of the N-terminal helix I and the recognition helix III for efficient binding of the Bcd-HD to its DNA target. Although Nanda and Brand (*35*) propose that an interaction between Phe or Tyr at position 8 and $Trp^{48}$ contributes to the low quantum yield of $Trp^{48}$, the tryptophan of the F8A mutant of the Bcd-HD is still considerably quenched (*9*).

Each homeodomain or mutant in Table 3 has a higher enthalpic contribution than the corresponding $-T\Delta S$ value at 298 K for the unfolding−folding equilibrium. Although the thermodynamic unfolding parameters at 298 K are similar for Nkx2.5(C56S) and the H52R mutant of vnd/NK-2 (Table 3), differences for NK-2(H52R) binding specific DNA are observed.

Thermodynamic parameters for HD binding specific 18 bp DNA at pH 7.4 (298 K) are compared in Table 4 for Nkx2.5(C56S) and wild-type vnd//NK-2 and mutants NK-2(H52R) and NK-2(H52R/T56W). The Nkx2.5(C56S) HD has the highest affinity constant at 298 K for DNA ($\Delta G' = -11.8$ kcal/mol). In all cases, the DNA binding reaction is enthalpically controlled, although significant entropic contributions to $\Delta G'$ for binding DNA ($-T\Delta S$) are observed for Nkx2.5(C56S), wild-type vnd/NK-2, and NK-2(H52R/T56W). The $-T\Delta S$ contribution may reflect the solvent involvement that is necessary for maximum efficiency in DNA binding. In the case of the lethal NK-2(H52R) mutation, the DNA binding affinity of NK-2(H52R) is lower than that of Nkx2.5 and the $-T\Delta S$ contribution is nearly zero which may reflect some subtle impairment of DNA binding. The importance of solvent involvement for homeodomain binding to DNA is demonstrated by the experiments of Damante et al. (*37*) with the TTF-1 HD, for which it has been found that physiological temperatures and salt concentrations favor specific binding to the 5′-CAAGTGT-3′ sequence with an affinity at least 1000-fold higher than that of binding a nonspecific DNA sequence.

The $\Delta C_p$ value for wild-type vnd/NK-2 binding specific DNA is positive (Table 4), meaning that the affinity for DNA decreases with an increase in temperature as $\Delta H$ becomes less negative. This may reflect the greater flexibility of the unbound vnd/NK-2 observed in Trp fluorescence studies in the absence and presence of 18 bp DNA (Figure 5). In contrast, the Trp fluorescence of Nkx2.5(C56S) is not affected by specific DNA binding at 25 °C, and the $\Delta C_p$ value is negative for Nkx2.5(C56S) binding 18 bp DNA. In the latter case, the binding enthalpy becomes more negative and the affinity for DNA increases with an increase in temperature. Thus, $-T\Delta S$ approaches zero as the temperature is increased to 37 °C (Figure 7), which marks the onset of unfolding (Figure 2), at least for the isolated HD. A longer

Table 4: Thermodynamic Parameters for Nkx2.5(C56S), NK-2, NK-2(H52R), and NK-2(H52R/T56W) Homeodomains Binding Specific 18 bp DNA at pH 7.4 and 298 K[a]

| protein | $K_A'$ ($\times 10^{-8}$ $M^{-1}$) | $\Delta H$ (kcal/mol) | $\Delta G'$ (kcal/mol) | $-T\Delta S$ (kcal/mol) | $\Delta C_p$ (kcal $K^{-1}$ $mol^{-1}$) |
|---|---|---|---|---|---|
| Nkx2.5(C56S) | $4.9 \pm 2.0$ | $-10.4 \pm 0.2$ | $-11.8 \pm 0.2$ | $-1.5 \pm 0.3$ | $-0.18 \pm 0.01$ |
| NK-2 | $1.2 \pm 0.1$ | $-6.6 \pm 0.5$ | $-11.0 \pm 0.1$ | $-4.4 \pm 0.5$ | $0.25 \pm 0.04$ |
| NK-2(H52R) | $1.2 \pm 0.2$ | $-10.8 \pm 0.1$ | $-11.0 \pm 0.1$ | $-0.2 \pm 0.1$ | $-0.17 \pm 0.01$ |
| NK-2(H52R/T56W) | $2.0 \pm 0.8$ | $-9.0 \pm 0.6$ | $-11.3 \pm 0.3$ | $-2.3 \pm 0.6$ | $-0.10 \pm 0.04$ |

[a] For Nkx2.5(C56S), titrations have been performed in 20 mM MOPS and 100 mM NaCl (pH 7.4). $K_A'$ is the average of two separate experiments at 298 K (Table 2), and $\Delta H$ and its error are from the linear least-squares fitting of $\Delta H$ values vs temperature (Figure 7). Values of $\Delta G'$ and $-T\Delta S$ with their errors are calculated using the equations specified in Materials and Methods based on the values and standard deviations of $K_A'$ and $\Delta H$. Values for wild-type NK-2 and its mutants are taken from Gonzalez et al. (*7*), whose measurements were taken in 50 mM sodium phosphate (pH 7.4). All of these HD proteins form a 1:1 complex with specific, duplex DNA.

construct containing the Nkx2.5 HD might be more stable due to protein−protein interactions with other transcription factors.

Using the relationship of Spolar et al. (*38*) for calculating nonpolar surface burial, the value of $\Delta C_p$ for Nkx2.5(C56S) binding specific DNA (Table 4) corresponds to $648 \pm 36$ Å$^2$ of apolar surface buried on binding DNA. NMR data have been used to calculate the difference in the apolar surface of free NK-2 and that for NK-2 bound to DNA at 12 °C to give an estimate of 625 Å$^2$ for the apolar surface burial on binding DNA (*23*). A similar calculation from NMR data gives a polar surface area of 329 Å$^2$ buried on NK-2 binding DNA. Using these apolar and polar surface areas buried on DNA binding, a $\Delta C_p$ value of $-0.15$ kcal $K^{-1}$ $mol^{-1}$ is calculated from eq 1 of Spolar and Record (*39*), which is somewhat less negative than that measured for Nkx2.5(C56S) and NK-2(H52R) but has a different sign compared to that measured for wild-type NK-2 (Table 4). The $\Delta C_p$ value of 0.25 kcal $K^{-1}$ $mol^{-1}$ for wild-type NK-2 binding DNA appears to be the result of an unusual solvent rearrangement and/or burial of ionic groups (*7*). It is possible that the burial or increased ordering of H52 is solely responsible for producing the energetic penalty during DNA binding by the vnd/NK-2 HD.

Tyr$^{54}$ of TTF-1 (*40*) and the NK-2 HD family (*41*) is the primary determinant for recognizing the 5′-CAAG-3′ nucleotide sequence at the fourth complementary position (i.e., the paired C). Gruschus et al. (*23*) have determined the three-dimensional structure of the vnd/NK-2 HD−DNA complex by NMR spectroscopy. Helix III of NK-2 binds in the major groove of B-DNA, and side chains of residues K46, I47, Q50, N51, R53, and Y54 have been identified as making close contacts with duplex DNA having at its core 5′-CAAGTG-3′. The positively charged N-terminal arm of the NK-2 HD interacts with the ribose phosphates of the B-DNA minor groove backbone as well as DNA bases via side chains of K3, R5, V6, L7, and F8 (*23*). These interactions are summarized here in an effort to better understand the enthalpically driven thermodynamics for the binding of specific DNA by both NK-2 and Nkx2.5.

Kasahara and Benson (*21*) have reported on the properties of eight NKX2.5 HD mutations (R5C, L34P, T41M, Q50H, N51K, R52G, R53H, and Y54C), located throughout the HD, that cause abnormalities in heart development. Although a spectrum of biochemical phenotypes has been identified, the best correlation with clinical phenotypes was found to be a markedly impaired DNA binding by the NKX2.5 mutants (*21*). From the NMR results (*23*), it can be predicted that the Y54C mutant will be impaired in DNA recognition and the other helix III mutants (Q50R, N51K, and R53H) all will be defective in binding to the major groove of sequence-specific B-DNA. The R5C mutant will be defective in binding to the B-DNA minor groove. It can be predicted also that the L34P mutant will have a distorted helix II, and since the T41M mutation is in the turn loop, neither mutant will have the optimal helix−turn−helix DNA binding motif. Thermodynamic results presented here suggest that the R52G mutant will be destabilized and temperature-sensitive since the ion pair interaction with Glu$^{17}$ will be missing. Destabilized mutants will be quickly degraded by endogenous proteases. It should be noted that Kasahara and Benson (*21*) have emphasized that in vivo the total dose of NKX2.5 capable of binding to DNA is critical.

In summary, the studies presented here give a comprehensive thermodynamic characterization of the unfolding/folding and specific duplex DNA binding of the Nkx2.5-(C56S) homeodomain. The energetics of folding and DNA binding previously have been determined for only two other homeodomains, MATα2 (*6*) and vnd/NK-2 (*7*). Although these three homeodomains have similar structures, the energetics of specific DNA binding differ significantly which can be attributed mainly to conformational differences in the unbound proteins.

## ACKNOWLEDGMENT

We thank Dr. Henry M. Fales for performing mass spectral analyses.

## REFERENCES

1. Ghering, W. J., Affolter, M., and Bürglin, T. (1994) Homeodomain proteins, *Annu. Rev. Biochem. 63*, 487−526.
2. Kim, Y., and Nirenberg, M. (1989) *Drosophila* NK-homeobox genes, *Proc. Natl. Acad. Sci. U.S.A. 86*, 7716−7720.
3. Damante, G., Fabbro, D., Pellizzari, L., Civitareale, D., Guazzi, S., Polycarpou-Schwartz, M., Caucci, S., Quadrifoglio, F., Formisano, S., and Di Lauro, R. (1994) Sequence-specific DNA recognition by the thyroid transcription factor-1 homeodomain, *Nucleic Acids Res. 22*, 3075−3083.
4. Wang, L. H., Chmelik, R., and Nirenberg, M. (2002) Sequence-specific DNA binding by the vnd/NK-2 homeodomain of *Drosophila*, *Proc. Natl. Acad. Sci. U.S.A. 99*, 12721−12726.
5. Chen, C. Y., and Schwartz, R. J. (1995) Identification of novel DNA binding targets and regulatory domains of a murine tinman homeodomain factor, Nkx2.5, *J. Biol. Chem. 270*, 15628−15633.
6. Carra, J. H., and Privalov, P. L. (1997) Energetics of folding and DNA binding of the MAT α2 homeodomain, *Biochemistry 36*, 526−535.
7. Gonzalez, M., Weiler, S., Ferretti, J. A., and Ginsburg, A. (2001) The vnd/NK-2 homeodomain: Thermodynamics of reversible unfolding and DNA binding for wild-type and with residue replacements H52R and H52R/T56W in helix III, *Biochemistry 40*, 4923−4931.

8. Damante, G., Tell, G., Leonardi, A., Fogolari, F., Bortolotti, N., Di Lauro, R., and Formisano, S. (1994) Analysis of the conformation and stability of rat TTF-1 homeodomain by circular dichroism, *FEBS Lett. 354*, 293−296.
9. Subramaniam, V., Jovin, T. M., and Rivera-Pomar, R. V. (2001) Aromatic amino acids are critical for stability of the bicoid homeodomain, *J. Biol. Chem. 276*, 21506−21511.
10. Weiler, S., Gruschus, J. M., Tsao, D. H., Yu, L., Wang, L. H., Nirenberg, M., and Ferretti, J. A. (1998) Site-directed mutations in the vnd/NK-2 homeodomain. Basis of variations in structure and sequence-specific DNA binding, *J. Biol. Chem. 273*, 10994−11000.
11. Frasch, M., Warrior, R., Tugwood, J., and Levine, M. (1988) Molecular analysis of *even-skipped* mutants in *Drosophila* development, *Genes Dev. 2*, 1824−1838.
12. Heberlein, U., Penton, A., Falsafi, S., Hackett, D., and Rubin, G. M. (1994) The C-terminus of the homeodomain is required for functional specificity of the *Drosophila rough* gene, *Mech. Dev. 48*, 35−49.
13. Laughon, A., and Scott, M. P. (1984) Sequence of a *Drosophila* segmentation gene: Protein structure homology with DNA-binding proteins, *Nature 310*, 25−31.
14. Hirsch, J. A., and Aggarwal, A. K. (1995) Structure of the even-skipped homeodomain complexed to AT-rich DNA: New perspectives on homeodomain specificity, *EMBO J. 14*, 6280−6291.
15. Bruneau, B. G. (2002) Transcriptional regulation of vertebrate cardiac morphogenesis, *Circ. Res. 90*, 509−519.
16. Zaffran, S., and Frasch, M. (2002) Early signals in cardiac development, *Circ. Res. 91*, 457−469.
17. Komuro, I., and Izumo, S. (1993) Csx: A murine homeobox-containing gene specifically expressed in the developing heart, *Proc. Natl. Acad. Sci. U.S.A. 90*, 8145−8149.
18. Schott, J. J., Benson, D. W., Basson, C. T., Pease, W., Silberbach, G. M., Moak, J. P., Maron, B. J., Seidman, C. E., and Seidman, J. G. (1998) Congenital heart disease caused by mutations in the transcription factor NKX2−5, *Science 281*, 108−111.
19. Benson, D. W., Silberbach, G. M., Kavanaugh-McHugh, A., Cottrill, C., Zhang, Y., Riggs, S., Smalls, O., Johnson, M. C., Watson, M. S., Seidman, J. G., Seidman, C. E., Plowden, J., and Kugler, J. D. (1999) Mutations in the cardiac transcription factor NKX2.5 affect diverse cardiac developmental pathways, *J. Clin. Invest. 104*, 1567−1573.
20. Goldmuntz, E., Geiger, E., and Benson, D. W. (2001) NKX2.5 mutations in patients with tetralogy of fallot, *Circulation 104*, 2565−2568.
21. Kasahara, H., and Benson, D. W. (2004) Biochemical analyses of eight NKX2.5 homeodomain missense mutations causing atrioventricular block and cardiac anomalies, *Cardiovasc. Res. 64*, 40−51.
22. Turbay, D., Wechsler, S. B., Blanchard, K. M., and Izumo, S. (1996) Molecular cloning, chromosomal mapping, and characterization of the human cardiac-specific homeobox gene hCsx, *Mol. Med. 2*, 86−96.
23. Gruschus, J. M., Tsao, D. H. H., Wang, L. H., Nirenberg, M., and Ferretti, J. A. (1999) The three-dimensional structure of the vnd/NK-2 homeodomain-DNA complex by NMR spectroscopy, *J. Mol. Biol. 289*, 529−545.
24. Perkins, S. J. (1986) Protein volumes and hydration effects. The calculations of partial specific volumes, neutron scattering match-points and 280-nm absorption coefficients for proteins and glycoproteins from amino acid sequences, *Eur. J. Biochem. 157*, 169−180.
25. Cantor, C. R., Warshaw, M. M., and Shapiro, H. (1970) Oligonucleotide interactions. III. Circular dichroism studies of the conformation of deoxyoligonucleotides, *Biopolymers 9*, 1059−1077.
26. Tsao, D. H., Gruschus, J. M., Wang, L. H., Nirenberg, M., and Ferretti, J. A. (1994) Elongation of helix III of the NK-2 homeodomain upon binding to DNA: A secondary structure study by NMR, *Biochemistry 33*, 15053−15060.
27. Lee, H. S., Gruschus, J. M., Zang, T., and Ferretti, J. A. (2005) Letter to the Editor: NMR assignments of the DNA-bound human Csx/Nkx2.5 homeodomain and NK-2-specific domain, *J. Biomol. NMR 31*, 75−76.
28. Gruschus, J. M., and Ferretti, J. A. (1999) Signal enhancement using 45 degrees water flipback for 3D N-15-edited ROESY and NOESY HMQC and HSQC, *J. Magn. Reson. 140*, 451−459.
29. Delaglio, F., Grzesiek, S., Vuister, G. W., Zhu, G., Pfeifer, J., and Bax, A. (1995) NMRPipe: A multidimensional spectral processing system based on UNIX pipes, *J. Biomol. NMR 6*, 277−293.
30. Perczel, A., Park, K., and Fasman, G. D. (1992) Analysis of the circular dichroism spectrum of proteins using the convex constraint algorithm: A practical guide, *Anal. Biochem. 203*, 83−93.
31. Kirchhoff, W. H. (1993) NIST Technical Note 1401: EXAM (CODEN: NTNOEF), U.S. Government Printing Office, Washington, DC.
32. Plotnikov, V. V., Brandts, J. M., Lin, L. N., and Brandts, J. F. (1997) A new ultrasensitive scanning calorimeter, *Anal. Biochem. 250*, 237−244.
33. Ginsburg, A., and Zolkiewski, M. (1991) Differential scanning calorimetry study of reversible, partial unfolding transitions in dodecameric glutamine synthetase from *Escherichia coli*, *Biochemistry 30*, 9421−9429.
34. Privalov, G. P., and Privalov, P. L. (2000) Problems and prospects in microcalorimetry of biological macromolecules, *Methods Enzymol. 323*, 31−62.
35. Nanda, V., and Brand, L. (2000) Aromatic interactions in homeodomains contribute to the low quantum yield of a conserved, buried tryptophan, *Proteins 40*, 112−125.
36. Slutsky, M., and Mirny, L. A. (2004) Kinetics of protein-DNA interaction: Facilitated target location in sequence-dependent potential, *Biophys. J. 87*, 4021−4035.
37. Damante, G., Tell, G., Formisano, S., Fabbro, D., Pellizzari, L., and Di Lauro, R. (1993) Effect of salt concentration on TTF-1 HD binding to specific and non-specific DNA sequences, *Biochem. Biophys. Res. Commun. 197*, 632−638.
38. Spolar, R. S., Ha, J.-H., and Record, M. T. (1989) Hydrophobic effect in protein folding and other noncovalent processes involving proteins, *Proc. Natl. Acad. Sci. U.S.A. 86*, 8382−8385.
39. Spolar, R. S., and Record, M. T. (1994) Coupling of local folding to site-specific binding of proteins to DNA, *Science 263*, 777−784.
40. Damante, G., Pellizzari, L., Esposito, G., Fogolari, F., Viglino, P., Tell, G., Formisano, S., and Di Lauro, R. (1996) A molecular code dictates sequence-specific DNA recognition by homeodomains, *EMBO J. 15*, 4992−5000.
41. Gruschus, J. M., Tsao, D. H. H., Wang, L.-H., Nirenberg, M., and Ferretti, J. A. (1997) Interaction of the vnd/NK-2 homeodomain with DNA by nuclear magnetic resonance spectroscopy: Basis of binding specificity, *Biochemistry 36*, 5372−5380.

BI050835S